Marine Research
of the National Academy of Marine Research
ISSN: 2709-6629 (Vol.4 Iss.2)
GPN: 2011200033

DOI: http://dx.doi.org/10.29677/MR.202412_4(2).0003
2024, 4(2), 30-54

Study on the Fluid Selection and System Efficiency of Ocean Thermal Energy Conversion Technology

Jhih-Han Chen [1] Yi-Hisang Yu [1*]

[1] *Department of Civil Engineering, National Yang Ming Chiao Tung University, Hsinchu, Taiwan*

ABSTRACT

Climate change has been scientifically established as an urgent global challenge with significant impacts, drawing substantial international attention. In response, many countries have committed to achieving "Net Zero Emissions by 2050" and are actively implementing policies to mitigate its effects. Ocean thermal energy conversion (OTEC) technology has emerged as a promising renewable energy source, capable of generating electricity by exploiting the temperature difference between warm surface seawater and cold deep seawater. This study aims to analyze the performance of a dual-stage organic Rankine cycle system, recognized as one of the promising configurations for OTEC applications due to its enhanced efficiency in utilizing temperature differentials. A sensitivity analysis was conducted on 13 different working fluids to evaluate the impact of critical parameters on system performance, including seawater pipe diameter, pinch point temperature, and working fluid mass flow rate. The analysis employed MATLAB simulations based on seawater surface temperature data from the Heping area in Hualien, Taiwan, where Taiwan Cement Corporation proposed a 1 MW OTEC plant. The study identified optimal design parameters for each working fluid, revealing significant performance variations. Finally, this study includes an economic analysis to evaluate the levelized cost of energy and the feasibility of deploying OTEC technology on a commercial scale. Although the overall cost of the OTEC system employing R134a (tetrafluoromethane, a type of refrigerant) is slightly higher than that of ammonia, the findings indicate that R134a outperforms ammonia in thermal efficiency and economic viability, particularly highlighting significant advantages in the back-work ratio and net power output of the OTEC system. The findings also suggest that, with appropriate system design and optimization, OTEC technology can provide a stable and sustainable power supply, making it a viable option for regions with suitable thermal gradients, such as the South China Sea and tropical island nations.

Keywords: ocean thermal energy conversion, working fluid, levelized cost of energy, double-stage organic Rankine cycle.

* Corresponding author, e-mail: yyu@nycu.edu.tw

Received October 4, 2024, accepted November 5, 2024.

1 INTRODUCTION

Energy is crucial for achieving social, economic, and environmental objectives while facilitating national economic activities. With ongoing economic development and population growth, energy consumption is rising rapidly. As illustrated in Figure 1, Taiwan's current electricity generation primarily depends on thermal power sources, including coal, oil, and natural gas, complemented by nuclear energy and renewable resources such as hydropower, solar energy, wind energy, and ocean energy, along with other generation methods like cogeneration (Taiwan Power Company, n.d.). To address rising energy demand and achieve the target of "Net Zero Emissions by 2050," it is crucial to actively promote the acceleration of energy transition toward renewable sources, including wind, solar, and ocean energy.

Ocean energy stands out among these renewable energy options due to its diverse potential, which includes wave energy, tidal energy, and a relatively unique technology known as ocean thermal energy conversion (OTEC). OTEC leverages the temperature difference between warm surface seawater and colder deep seawater to generate electricity. Demonstration plants have been built and continue to operate, including the Makai OTEC plant in the United States (Makai Ocean Engineering, 2015) and one in Okinawa, Japan (OTEC Okinawa, n.d.), each with a capacity of approximately 100 kW.

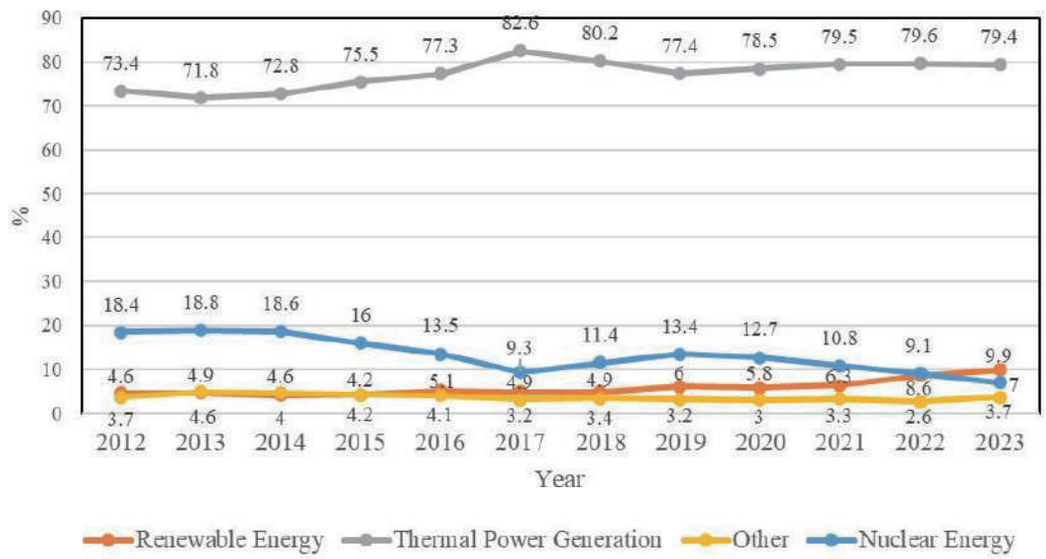

Figure 1. Taiwan's power generation structure from 2012 to 2023. (Taiwan Power Company, n.d.)

The efficiency of OTEC systems largely depends on the temperature differential between warm surface water and cold deep water. There are three main types of OTEC systems: open-cycle (Figure 2a), closed-cycle (Figure 2b), and hybrid-cycle, incorporating elements of both open and closed systems. Table 1 shows the principles of open and closed circulation systems. One of the main challenges for OTEC systems is their relatively low thermal efficiency in the Rankine cycle, typically between 3% and 5%, which is significantly lower than that of conventional thermal power plants. Several alternative thermal cycles have been proposed to address these efficiency limitations, such as the Kalina cycle, the organic Rankine cycle, and the dual-stage Rankine cycle (Chen & Huo, 2023). The selection of the working fluid in these systems is critical, as it impacts thermodynamic efficiency and involves considerations such as toxicity, environmental sustainability, and cost.

Marine Research of the National Academy of Marine Research
DOI: 10.29677/MR.202412_4(2).0003

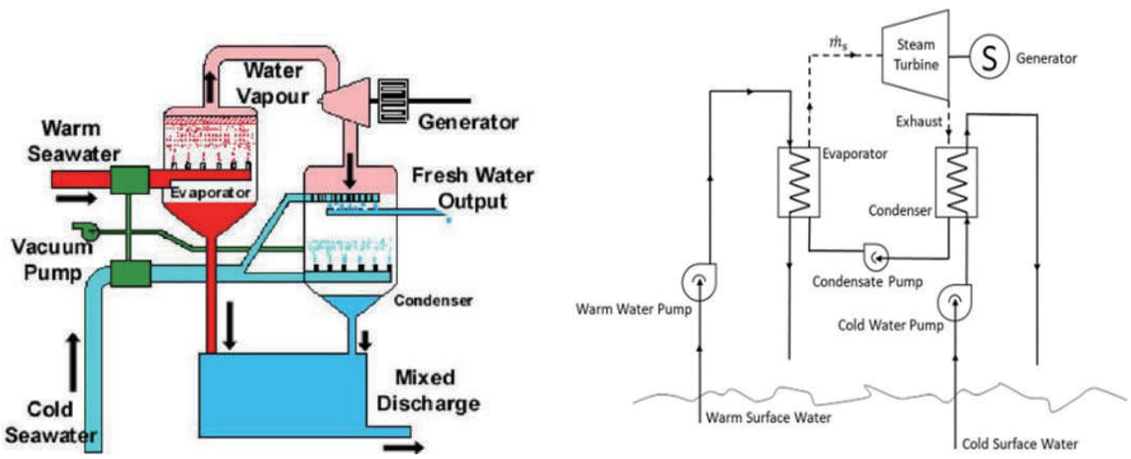

(a) Open-cycle (Renewable Energy Sources, 2009) (b) Closed-cycle (Gu, 2023)

Figure 2. Schematic diagrams of OTEC systems.

Table 1. Principles of open-cycle and closed-cycle systems. (Kempener & Neumann, 2014)

	Open-cycle	Closed-cycle
Operating principles	• The system uses seawater as a working medium. Warm surface seawater is drawn into a vacuum evaporator, where it rapidly flashes into steam under vacuum conditions. • The generated steam is transported through pipelines to a turbine, driving it to rotate and generate electricity via a generator. • The steam exiting the turbine enters a condenser, cools, and condenses into freshwater. This freshwater can be discharged back into the ocean or processed for direct use as drinking water; it does not return to the evaporator.	• The system uses a liquid working fluid (such as ammonia or other low-boiling liquids) as a medium. Warm surface seawater heats the working fluid in an evaporator, causing it to evaporate into steam. • The generated steam is transported through pipelines to a turbine, which converts thermal energy into mechanical energy, driving a generator to produce electricity. • The steam is cooled in a condenser by deep seawater, condensing back into liquid working fluid, which is then recycled for reuse.

Historically, closed-cycle OTEC systems have used R717 (ammonia) due to its low boiling point. However, as the phase-out of ozone-depleting substances like R22 progressed, alternative refrigerants such as R32, R125, R134a, and R410a were explored (Kim et al., 2009). Saleh et al. (2007) examined 31 fluids, finding that balancing thermodynamic properties with safety considerations is crucial. Yoon et al. (2014) evaluated various working fluids (refrigerants) and noted that R717 and R245fa demonstrated high thermal efficiency among wet and isentropic fluids, respectively. The chemical properties of these working fluids are listed in Table 2.

DOI: 10.29677/MR.202412_4(2).0003

Further studies, such as those by Dijoux et al. (2017), evaluated R717, R507a, and R1234yf based on their thermodynamic performance and environmental impact. Alkhalidi et al. (2014) emphasized the efficiency of isobutane in OTEC applications, while Halimi and Atolah (2019) pointed out that butene could significantly improve thermal efficiency, achieving rates of up to 6.01%. In a subsequent study, Halimi et al. (2020) identified ammonia, butane, isobutane, and isobutene as optimal working fluids, each offering distinct advantages depending on performance and safety requirements.

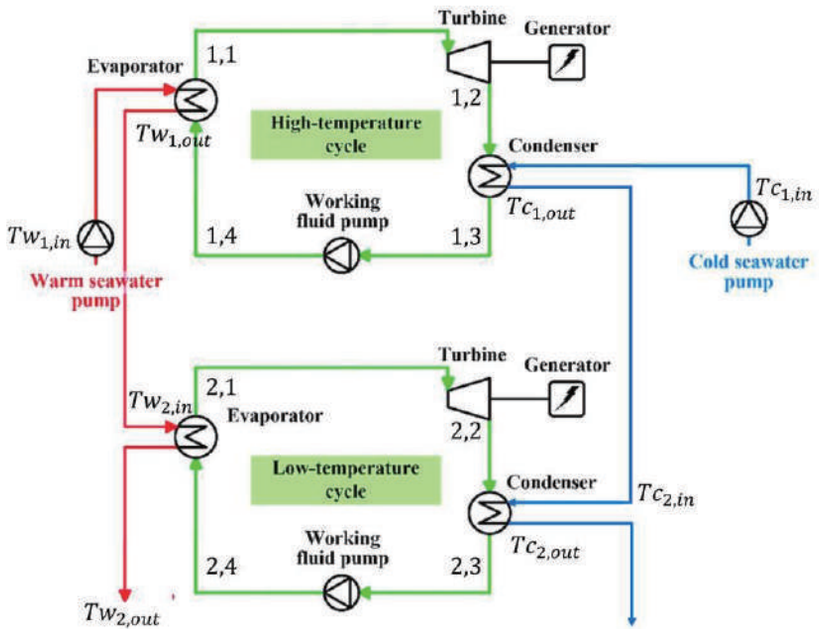

Figure 3. DORC model. (inspired by Ikegami et al. (2018))

Although ammonia is widely used for its efficiency and availability, it poses significant safety risks due to its toxicity and corrosiveness. In comparison, isobutane not only offers higher energy conversion efficiency but also serves as a safer alternative in terms of handling and environmental impact. Existing research on the efficiency of OTEC systems and the selection of working fluids highlights a persistent challenge in identifying a viable alternative to ammonia. Figure 3 presents a schematic diagram of a double-stage organic Rankine cycle OTEC system. In general, DORC configurations have the advantage of enhanced efficiency in utilizing temperature differentials. Kusuda et al. (2015) implemented an experimental DORC within an OTEC configuration, revealing that the DORC system could potentially achieve greater energy output compared to the traditional single-stage organic Rankine cycle (ORC). However, this system was used solely for experimental purposes, with no measurements of actual power output or thermal efficiency.

Thus, this study aims to further evaluate the DORC OTEC configuration and explore the potential alternative working fluids for their impact on the levelized cost of energy (LCOE). In particular, we assessed the OTEC thermodynamic performance and cost-efficiency, taking into account both initial installation and operational costs. The paper begins with model methodology and performance evaluation parameters, followed by a set of validation studies for three working fluids. The study also examines the impact of system parameters, including seawater flow rate and pipe diameter, on overall OTEC performance, concluding with an LCOE analysis.

Marine Research of the National Academy of Marine Research
DOI: 10.29677/MR.202412_4(2).0003

2 RESEARCH METHODS

2.1 Model Introduction

This study employs a DORC system as the cycle model, as shown in Figure 3. Each of the two cycles consists of four key components: a working fluid pump, a turbine generator, an evaporator, and a condenser. The deep cold seawater temperature is calculated using the formula provided in Liponi et al. (2022), which is given as:

$$T_c = -2.85 \times 10^{-8} z^3 + 7.91 \times 10^{-5} z^2 - 7.47 \times 10^{-2} z + 29.35 \quad (1)$$

where the cold seawater temperature, T_c, is represented as a fitting function of depth ($z > 0$), with depth measured in meters.

2.2 Mathematical Model

The mathematical model is established under several key assumptions. First, the system is assumed to operate under steady-state conditions, maintaining constant temperature, pressure, and flow rate throughout. Furthermore, variations in the kinetic and potential energy of the fluids are considered negligible, with uniform fluid velocities assumed across the system. Lastly, thermal losses within the seawater pipeline and related circulation processes are neglected, treating seawater as an incompressible fluid for simplification.

This study adopts a flooded evaporator, where the working fluid is in a saturated vapor state at the evaporator outlet and condenses into a saturated liquid state at the condenser outlet. Here, the pressure at various points in the OTEC cycle corresponds to either the evaporation pressure (P_1 and P_4) or the condensation pressure (P_2 and P_3). The following formulas are based on those presented in Yang et al. (2022).

2.2.1 Heat exchanger: Evaporator and condenser

In OTEC systems, the evaporator and condenser serve as the primary heat exchangers, where the working fluid undergoes phase changes by absorbing and releasing heat. The evaporator is where the working fluid absorbs heat from the warm surface seawater, evaporating into a saturated vapor state. The energy balance equation for the evaporator can be expressed as:

$$Q_e = \dot{m}_{\mathrm{wf}}(h_1 - h_4) = m_{\mathrm{ws}} C_{\mathrm{pe}} (T_{\mathrm{wsi}} - \Delta T_w - T_e) \quad (2)$$

where Q_e is the heat transfer rate in the evaporator, $\dot{m}_{\mathrm{wf}}$ is the mass flow rate of the working fluid, h_1 and h_4 are the specific enthalpies of the working fluid at different states, m_{ws} is the mass flow rate of the surface seawater, C_{pe} is the specific heat capacity of the surface seawater in the evaporation section, T_{wsi} is the surface seawater temperature at the evaporator inlet, T_e is the evaporator temperature, and ΔT_w is the evaporator pinch temperature.

Similarly, the condenser is where the working fluid releases heat to the cold deep seawater, condensing back into a saturated liquid state. The energy balance equation for the condenser is:

$$Q_c = \dot{m}_{\mathrm{wf}}(h_2 - h_3) = m_{\mathrm{cs}} C_{\mathrm{pc}} (T_c - \Delta T_c - T_{\mathrm{csi}}) \quad (3)$$

where Q_c is the heat transfer rate in the condenser, h_2 and h_3 are the specific enthalpies of the working fluid at different states, m_{cs} is the mass flow rate of the cold seawater, C_{pc} is the specific heat capacity of the cold seawater in the condensation section, T_{c} is the condenser temperature, T_{csi} is the cold seawater temperature at the condenser inlet, and ΔT_c is the condenser pinch temperature.

Marine Research of the National Academy of Marine Research
DOI: 10.29677/MR.202412_4(2).0003

These equations highlight the similarity in the energy balance approach for both heat exchangers, where the heat transfer rate depends on the mass flow rate, the change in specific enthalpy of the working fluid, and the temperature differences in the seawater streams.

2.2.2 Pump and power output

In OTEC systems, three main pumps are used: the working fluid pump, the warm seawater pump, and the cold seawater pump. The work done by the working fluid pump can be expressed as:

$$W_{p,wf} = \frac{\dot{m}_{\mathrm{wf}} \times \upsilon_4 (P_4 - P_3)}{\eta_{p,wf}} \tag{4}$$

where υ_4 is the specific volume of the working fluid and $\eta_{p,wf}$ is the working fluid pump efficiency. Similarly, the work required for the surface seawater pump is given by:

$$W_{\mathrm{p,ws}} = \frac{m_{\mathrm{ws}} \times \Delta P_w}{\rho_w \eta_{p,sw} \eta_g} \tag{5}$$

where ΔP_w is the surface seawater pipeline friction loss, ρ_w is the density of the seawater, $\eta_{p,sw}$ is the working fluid pump efficiency, and η_{g} is the generator efficiency. Likewise, the work done by the deep seawater pump is expressed as:

$$W_{\mathrm{p,cs}} = \frac{m_{\mathrm{cs}} \times \Delta P_c}{\rho_w \eta_{p,sw} \eta_g} \tag{6}$$

where ΔP_c is the deep seawater pipeline friction loss. The turbine expands the working fluid to perform work. The output power of the turbine can be calculated as:

$$W_t = \dot{m}_{\mathrm{wf}} \cdot (h_1 - h_2) \eta_g \tag{7}$$

where W_t is the work output of the turbine. The net power output of the DORC system is determined by balancing the input and output power of each component:

$$W_{net} = W_t - W_{\mathrm{p,wf}} - W_{\mathrm{p,ws}} - W_{\mathrm{p,cs}} \tag{8}$$

2.3 Performance Parameters

In this study, the performance of the OTEC system was evaluated using several key metrics based on Yang et al. (2022), as described below:

Net power per unit heat exchange area: Net power output per unit area refers to the amount of net power produced relative to the system's occupied space,

$$\gamma = \frac{W_{net}}{A_e + A_c} \tag{9}$$

where A_e and A_c are the areas of the evaporator and condenser, respectively. This metric is essential for evaluating spatial efficiency, particularly when installation space is constrained.

Exergy efficiency: Exergy efficiency measures how well a system uses input energy, accounting for energy quality and irreversibilities.

$$\eta_{ex} = \frac{W_{net}}{E_{xwi} + E_{xci}} \tag{10}$$

where E_{xwi} and E_{xci} are the available energy absorbed by the OTEC system from surface seawater and extracted from deep cold seawater, respectively.

Marine Research of the National Academy of Marine Research
DOI: 10.29677/MR.202412_4(2).0003

OTEC thermal efficiency: OTEC thermal efficiency is the ratio of net power output to total thermal input, as shown below,

$$\eta_{OTEC} = \frac{W_{net}}{Q_e} \tag{11}$$

Net output power per unit of seawater flow rate: Net power output per unit seawater flow rate measures the system's net power generated per unit of seawater flow, which is given as:

$$\mathrm{WPSF} = \frac{W_{net}}{m_w + m_c} \tag{12}$$

where m_w and m_c are the flow rates of surface and deep seawater, respectively. This metric helps assess the impact of seawater flow on system performance.

Back work ratio: The back work ratio (BWR) is the power used by auxiliary equipment (pumps) relative to the system's total output. A lower ratio indicates higher net power output, which is essential for system efficiency and economics. The formula can be given as:

$$\mathrm{BWR} = 1 - \frac{W_{net}}{W_t} \tag{13}$$

2.4 Economic Model

To assess the economic feasibility of the OTEC system, the levelized cost of energy (LCOE) was calculated, excluding costs associated with maritime operations, such as offshore installation, transportation, and decommissioning. The initial investment comprises capital expenditures for key OTEC components, including heat exchangers, pumps, turbines, and the evaporator, with adjustments based on equipment type, system pressure, and material selection.

The capital costs for heat exchangers, pumps, and turbines are estimated using the equipment module cost estimation techniques developed by Turton et al. (2009), which utilize standard engineering models to account for equipment and configuration variability. Furthermore, the cost of seawater pipes is based on the study by Langer et al. (2022), priced at 9 USD/kg, while the generator cost is determined using the formula proposed by Toffolo et al. (2014), as follows:

$$Cost_{generator} = 1.85 \times 10^6 \left(\frac{W_{net}[kW]}{11800}\right)^{0.94} \tag{14}$$

The total capital expenditure (CapEx) is calculated as:

$$Cost_{\mathrm{CapEx}} = Cost_{\mathrm{equ}} + Cost_{\mathrm{pipes}} + Cost_{\mathrm{generator}} \tag{15}$$

The capital recovery factor (CRCF) accounts for the interest rate (Ir) and lifetime (Lt) and is given by:

$$\mathrm{CRCF} = \frac{I_r(1+I_r)^{Lt}}{(1+I_r)^{Lt}-1} \tag{16}$$

For this study, an interest rate of 7% (Ir = 0.07) and a factory lifetime of 25 years (Lt = 25) were used. The LCOE is then calculated as:

$$\mathrm{LCOE} = \frac{CRCF \times Cost_{\mathrm{CapEx}} + C_{\mathrm{OM}}}{W_{\mathrm{net}} \times 8766(Hrs) \times \epsilon} \tag{17}$$

where C_{OM} is the annual operation and maintenance costs, approximated at 1.5% of the total capital cost, and η_{avail} is the device availability, assumed to be 95%.

Marine Research of the National Academy of Marine Research
DOI: 10.29677/MR.202412_4(2).0003

Table 2. Working fluid performance parameters.

Working fluid	Chemical property	Boiling temperature	Critical temperature	ODP	GWP	Security level
R125	Pentafluoroethane	-48.1˚C	66.02˚C	0	2,800	A1
R134a	Tetrafluoroethane	-26.1˚C	101.06˚C	0	1,300	A1
R717	Ammonia	-33.3˚C	132.25˚C	0	0	A3
R143a	Trifluoroethane	-47.2˚C	72.7˚C	0	3,800	A2L
R32	Difluoromethane	-51.7˚C	78.1˚C	0	675	A2L
R245fa	Pentafluoropropane	15.1˚C	154.0˚C	0	1,030	B1
R1234yf	tetrafluoroprop-1-ene	-29.5˚C	94.7˚C	0	4	A2L
Isoburane	Isoburane	-11.8˚C	134.7˚C	0	3	A3
butane	butane	-0.5˚C	152.0˚C	0	3	A3
R161	fluoroethane	-37.6˚C	102.2˚C	0	12	A3
R404a	52% Trifluoroethane /44% Pentafluoroethane /4% Tetrafluoroethane	-46.2˚C	72.1˚C	0	3,850	A1
R410a	50% Difluoromethane /50% Pentafluoroethane	-51.4˚C	71.3˚C	0	1,730	A1
R507a	50% Trifluoroethane /50% Pentafluoroethane	-46.7˚C	70.6˚C	0	3,985	A1

Table 3. Toxicity and flammability classification.

Flammability	Low toxicity	High toxicity
Non-flammable	A1	B1
Mildly flammable	A2L	B2L
Flammable	A2	B2
Highly flammable	A3	B3

Marine Research of the National Academy of Marine Research
DOI: 10.29677/MR.202412_4(2).0003

2.5 Working Fluid Performance Parameters

This study utilizes REFPROP 9.1 software (Lemmon et al., 2013) to analyze the working fluids mentioned in the literature, with the results presented in Table 2. The input parameters include ODP (ozone depletion potential), which measures a chemical's ability to deplete ozone, with higher values indicating a greater potential for ozone depletion, and GWP (global warming potential), which quantifies the impact of gas on global warming over 100 years, using CO_2 as a baseline with a value of 1. Safety classification is also considered, with substances categorized based on toxicity (Class A for low toxicity, Class B for high toxicity) and flammability (ranging from Class 1 to 3, with A1 being the safest and B3 the most hazardous). Further details on these classifications can be found in Table 3.

3 MODEL VALIDATION

This section presents a set of validation studies for the OTEC system model developed in this study. The model's accuracy and reliability are assessed by comparing the simulation results with existing literature data for different working fluids. This validation ensures that the model can be used to predict the performance of OTEC systems under various operating conditions.

3.1 Working Fluid - R134a

The validation process began with a comparative analysis of our model's performance relative to the work of Yang et al. (2022), who optimized the organic Rankine cycle design for OTEC systems utilizing R134a as the working fluid. Essential parameters, including evaporator and condenser temperatures, pinch point tempera tures, and working fluid flow rates, were established based on Yang et al.'s findings, as shown in Table 4. Our simulation results for R134a aligned with those reported by Yang et al., as illustrated in Figure 4, affirming our model's validity for this particular working fluid.

Table 4. R134a parameters.

Parameter	Symbol	Value
Surface seawater temperature	T_{wsi}	28°C
Deep seawater temperature	T_{csi}	4°C
Working fluid flowrate	m_{wf}	7.117kg/s
Seawater pump efficiency	ηP_{sw}	80%
Working fluid pump efficiency	ηP_{wf}	60%
Turbine efficiency	η_t	80%
Generator efficiency	η_g	90%
Pipeline diameter	d_w	0.35m
Surface seawater pipe length	l_w	200m
Deep seawater pipe length	l_c	3,000m

Marine Research of the National Academy of Marine Research
DOI: 10.29677/MR.202412_4(2).0003

Figure 4 illustrates the influence of seawater salinity on the system's performance. In this study, a salinity level of 35 practical salinity units (PSU) was adopted to ensure the model's accuracy. As seawater flow rates increase, variations in specific heat capacity can impact net power output and alter the size requirements of the evaporator and condenser. Higher flow rates enhance heat transfer efficiency, thereby improving the system's overall thermodynamic performance.

3.2 Working Fluid - Ammonia (R717)

Ammonia (R717) is widely used as a working fluid in OTEC systems due to its advantageous thermodynamic properties. By replicating the operating conditions established in the relevant literature (Yang & Yeh, 2022), the model showed a high degree of accuracy in reproducing trends in power output and efficiency, as shown in Table 5. Despite its potential advantages, safety concerns restrict the broader application of ammonia.

Table 5. R717 parameters.

Parameter	Symbol	Value
Surface seawater temperature	T_{wsi}	28°C
Deep seawater temperature	T_{csi}	5°C
Seawater flowrate	m_{ws}	200kg/s
Working fluid flowrate	m_{wf}	2.02kg/s
Seawater pump efficiency	ηP_{sw}	80%
Working fluid pump efficiency	ηP_{wf}	80%
Turbine efficiency	η_t	80%
Generator efficiency	η_g	80%
Pipeline diameter	d_w	2.5m
Surface seawater pipe length	l_w	250m
Deep seawater pipe length	l_c	2,800m

As illustrated in Figure 5, the discrepancy between the model's results and the literature is limited to within 5%. It is important to note that different studies may employ varied models and parameters, with simplified models often exhibiting greater errors. Furthermore, this study does not specify certain parameters, such as the diameter of the working fluid pipes, the number of pipes, seawater density, and the pipe roughness coefficient. Consequently, the parameters from Section 3.1 were applied in this investigation. Although these adjustments may introduce minor variations in net power output, the overall results remain within an acceptable range.

Marine Research of the National Academy of Marine Research
DOI: 10.29677/MR.202412_4(2).0003

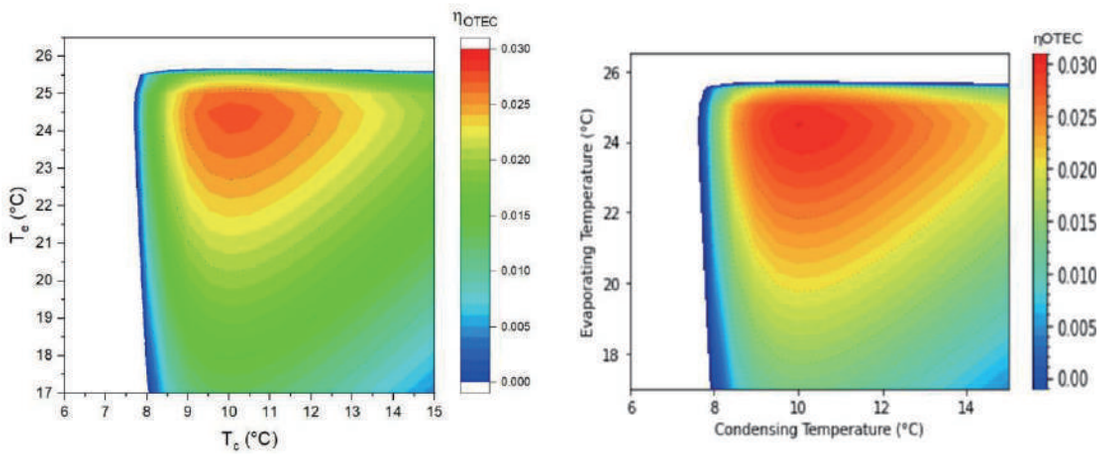

Literature: Yang et al. (2022) (Model output)

(a) Thermal efficiency of OTEC

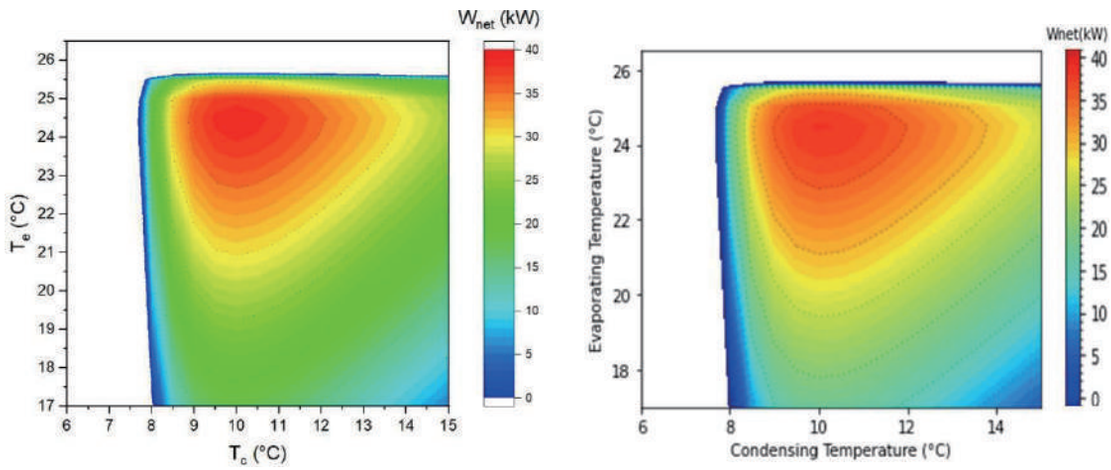

Literature: Yang et al. (2022) (Model output)

(b) Net output power

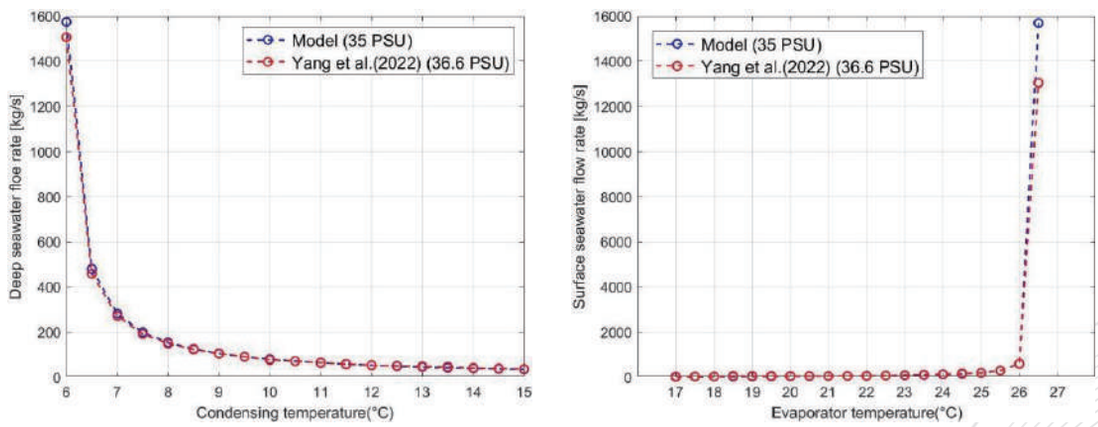

(c) Deep seawater flow rate (d) Surface seawater flow rate

Figure 4. Comparison of R134a literature and model.

DOI: 10.29677/MR.202412_4(2).0003

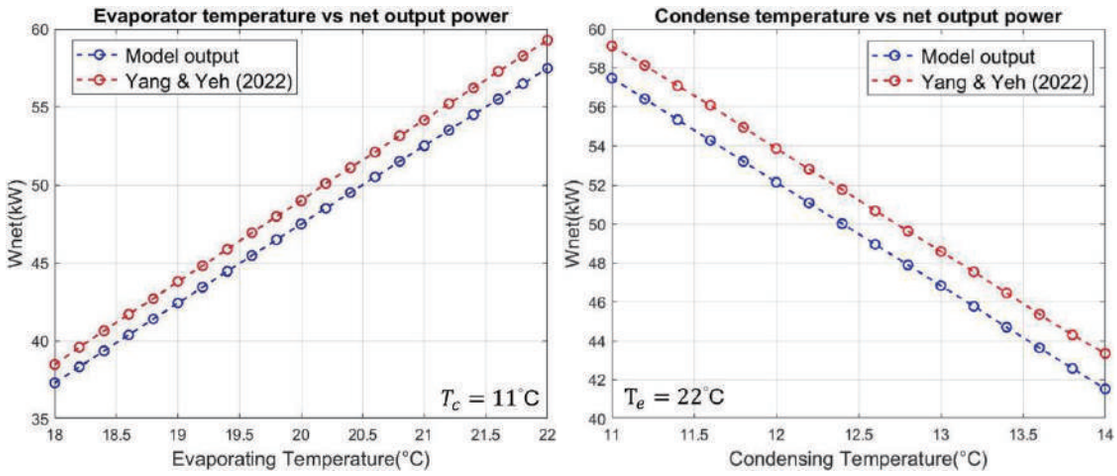

Figure 5. Comparison of R717 literature and model.

3.3 Working Fluid - R152a

For further validation, R152a was also investigated. Consistent with the previous working fluids, system parameters were adjusted based on existing literature to simulate an OTEC cycle utilizing R152a, with the parameters shown in Table 6 (Yang & Yeh, 2014). As observed in Figure 6, there are some discrepancies between the model outputs and the results reported in the literature. These differences may arise from variations between the model assumptions and actual system conditions, such as heat losses and pressure drops; however, they are within 5%.

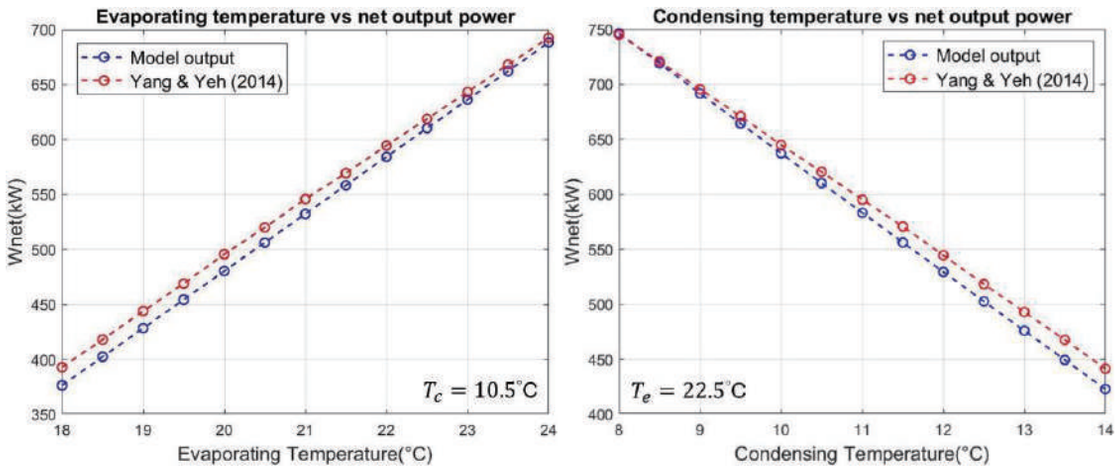

Figure 6. Comparison of R152a literature and model.

The three validation studies confirm that the net power output can be accurately calculated for any working fluid. Furthermore, this model incorporates various parameters, such as evaporator area, condenser area, and seawater flow rate, to estimate construction costs and serve as a tool for further research.

Marine Research of the National Academy of Marine Research
DOI: 10.29677/MR.202412_4(2).0003

Table 6. R152a parameters.

Parameter	Symbol	Value
Surface seawater temperature	T_{wsi}	28°C
Deep seawater temperature	T_{csi}	5°C
Seawater flowrate	m_{wf}	2,000kg/s
Seawater pump efficiency	ηP_{sw}	80%
Working fluid pump efficiency	ηP_{wf}	80%
Turbine efficiency	η_t	90%
Generator efficiency	η_g	90%
Surface seawater pipe length	l_w	100m
Deep seawater pipe length	l_c	750m

4 CASE STUDY

4.1 Reference Site

This study focuses on the Heping region of Hualien, Taiwan, as shown in Figure 7a, where Taiwan Cement Corporation plans to develop a 1 MW OTEC plant. Figure 7b presents the average sea surface temperatures in Heping from 2004 to 2023 (Central Weather Administration, 2024), including the maximum, average, and minimum temperatures. This data can be used to analyze monthly temperature variations, enabling the assessment of net power output fluctuations under different climatic conditions. To compare the performance of different working fluids, this analysis adopts standardized setup parameters, including a seawater pipeline length of 1,600 m and a depth of 600 m, based on specifications provided by Taiwan Cement Corporation (Wei, 2023).

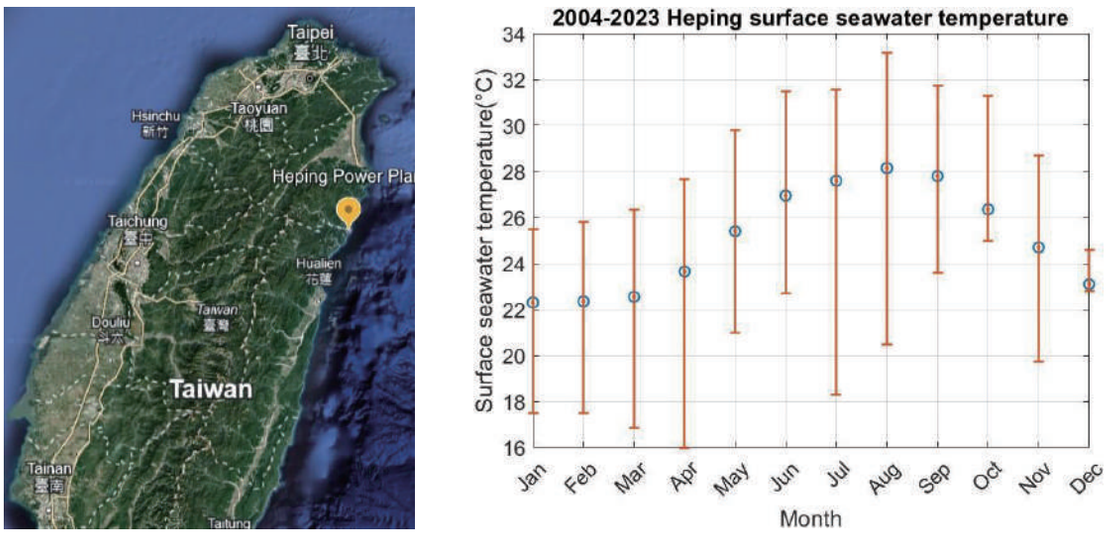

(a) Heping Power Company location

(b) Heping surface seawater temperature (Central Weather Administration, 2024)

Figure 7. Heping area information.

DOI: 10.29677/MR.202412_4(2).0003

4.2 Parametric Study

This section evaluates the effects of pinch point temperature, seawater pipeline diameter, and working fluid mass flow rate on system performance. It focuses on their specific impacts on energy output and efficiency, offering insights for optimizing system design and performance.

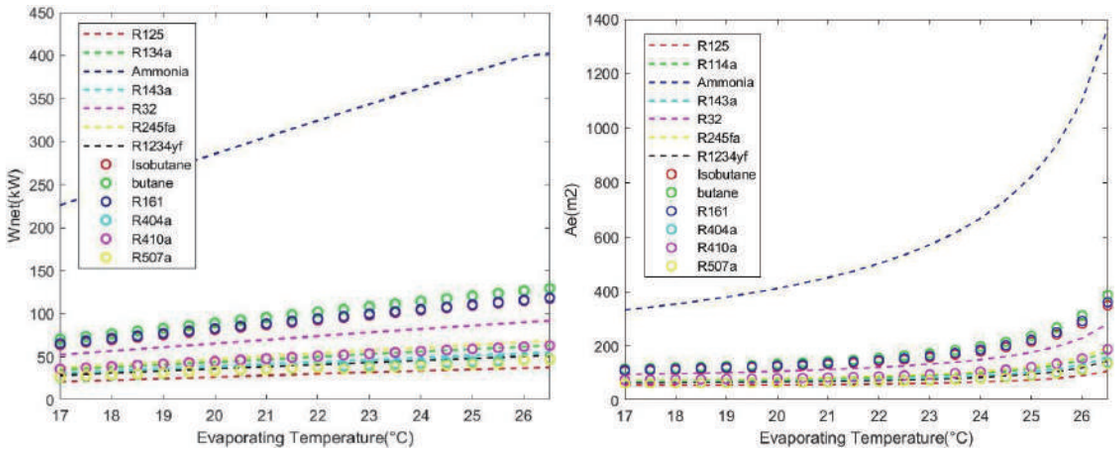

(a) $\Delta Te = \Delta Tc = 1.0°C$

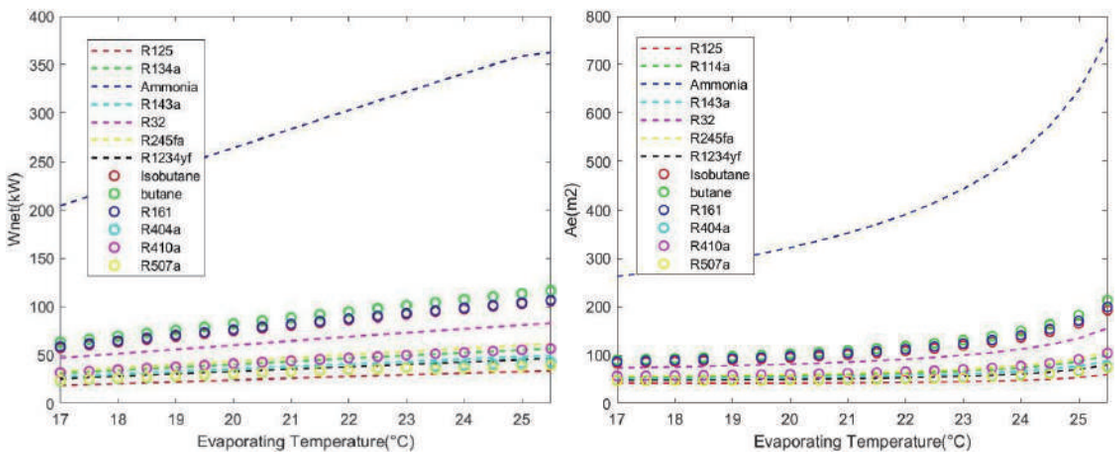

(b) $\Delta Te = \Delta Tc = 2.0°C$

Marine Research of the National Academy of Marine Research
DOI: 10.29677/MR.202412_4(2).0003

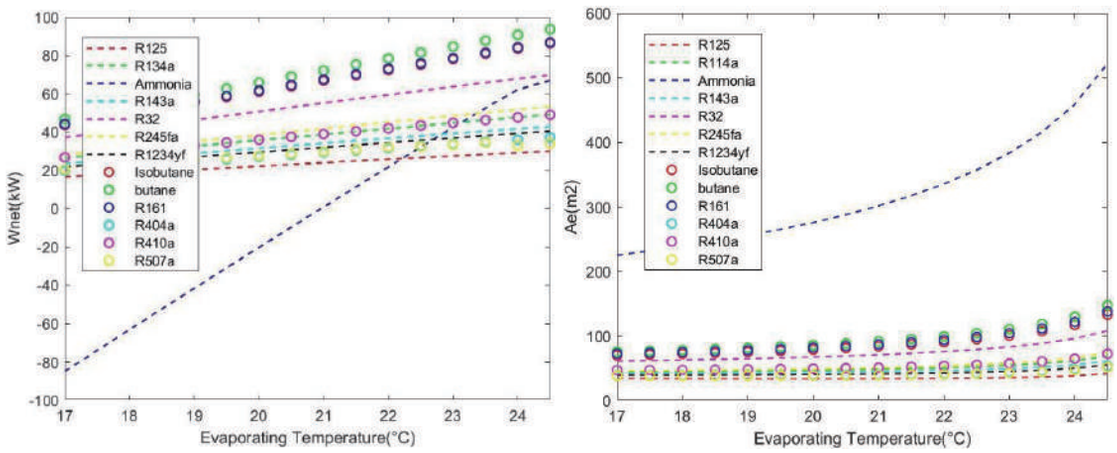

(c) $\Delta Te = \Delta Tc = 3.0°C$

Figure 8. The effect of different pinch point temperatures on net power (left) and the evaporator area (right).

4.2.1 Pinch point temperature

The pinch point temperature is crucial in OTEC system design, as it defines the minimum temperature difference between the working fluid and seawater. It affects heat transfer efficiency and the thermodynamic cycle, impacting the sizing of the evaporator and condenser, as well as overall energy conversion efficiency.

In the evaporator, the pinch point is the smallest temperature difference between the working fluid's evaporation and seawater temperatures. A lower pinch point enhances heat transfer efficiency but requires a larger heat exchanger area, significantly increasing capital costs. Similarly, the pinch point in the condenser represents the minimum temperature difference between the condensation temperature of the working fluid and the seawater temperature. Although a smaller pinch point improves heat exchange efficiency, it also necessitates larger heat exchanges. Thus, a careful balance between efficiency and cost is required.

Selecting an appropriate pinch point temperature is essential for balancing thermal efficiency and equipment costs in OTEC systems. For example, with a seawater temperature of 28°C, a pinch point of 0.5°C requires the working fluid's evaporation temperature to stay below 27.5°C. However, an overly small pinch point may reduce power generation.

As shown in Figure 8, reducing the pinch point temperature increases the required heat exchange area in the evaporator. This occurs because a smaller temperature difference reduces the heat transfer driving force, necessitating a larger surface area to maintain the desired heat exchange. However, a smaller pinch point reduces irreversibilities, thereby improving overall thermal efficiency. Conversely, a larger pinch point increases the driving force, reducing the required heat exchanger area but increasing irreversible losses, ultimately lowering system efficiency.

Marine Research of the National Academy of Marine Research
DOI: 10.29677/MR.202412_4(2).0003

4.2.2 Seawater pipeline diameter

The diameter of the seawater pipe significantly affects the system's flow rate, pressure drop, and energy conversion efficiency. A thorough understanding of the interaction between these variables is essential for effective pipeline design. This study evaluates system performance within a fixed evaporator temperature range of T_e = 17~26°C. The analysis of the seawater pipe diameter's impact on system performance, as shown in Figure 9, reveals two key findings.

For ammonia as the working fluid, an increase in evaporation temperature initially enhances net power output, followed by a subsequent decline. Smaller pipe diameters improve heat exchange efficiency by facilitating more effective interaction between seawater and the working fluid, thereby enhancing heat transfer. However, due to ammonia's higher viscosity, increased flow rates result in greater friction along the pipe walls, which reduces power output. In contrast, working fluids with lower viscosity can maintain higher flow rates without significant performance losses.

While smaller pipe diameters may be sufficient for lower flow rates, larger diameters are required at higher flow rates to reduce pressure losses and maintain system efficiency. Consequently, at identical pipe diameters, increasing the flow rate of ammonia has a more significant impact on system performance compared to lower-viscosity fluids (i.e., R134a, R410a, R507a).

4.2.3 Working fluid mass flow rate

Variations in the mass flow rate of the working fluid significantly influence the heat transfer rates within the evaporator and condenser, thereby affecting overall system performance. An insufficient flow rate can reduce heat exchange efficiency, while an excessively high flow rate may result in increased operational costs and energy consumption. As shown in Figure 10, when ammonia is used as the working fluid, substantial fluctuations in net power output are observed with a seawater pipe diameter of 2.0 m. Specifically, when the mass flow rate exceeds 15 kg/s, the net power output decreases at elevated temperatures and may even become negative at lower temperatures. This suggests that a larger seawater pipe diameter would be necessary to achieve a net power output of 1 MW. In contrast, for other working fluids, the net power output increases steadily as the flow rate rises, maintaining stability across both high- and low- temperature conditions. However, the increase in flow rate necessitates a larger evaporator size, which underscores the importance of optimizing parameter settings to balance economic feasibility with the desired power output.

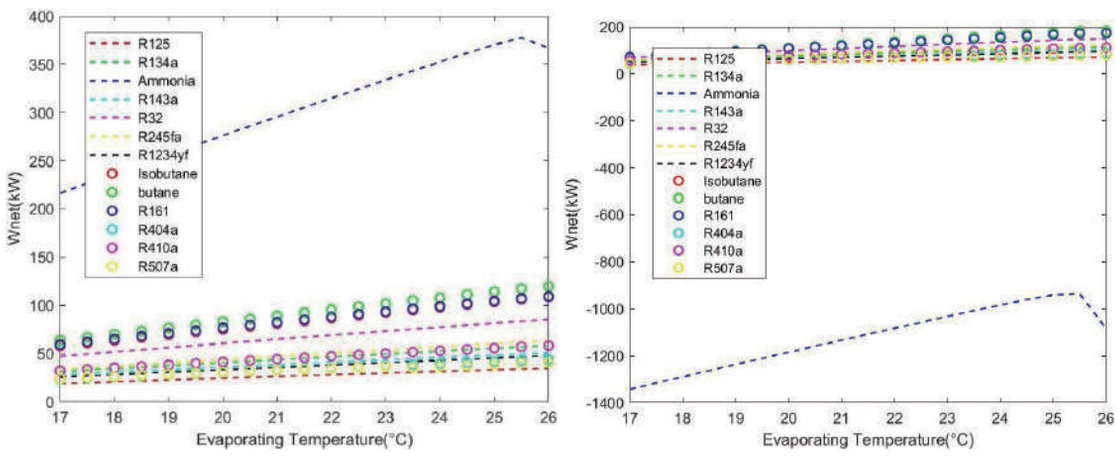

(a) d_w = 1.5 m

DOI: 10.29677/MR.202412_4(2).0003

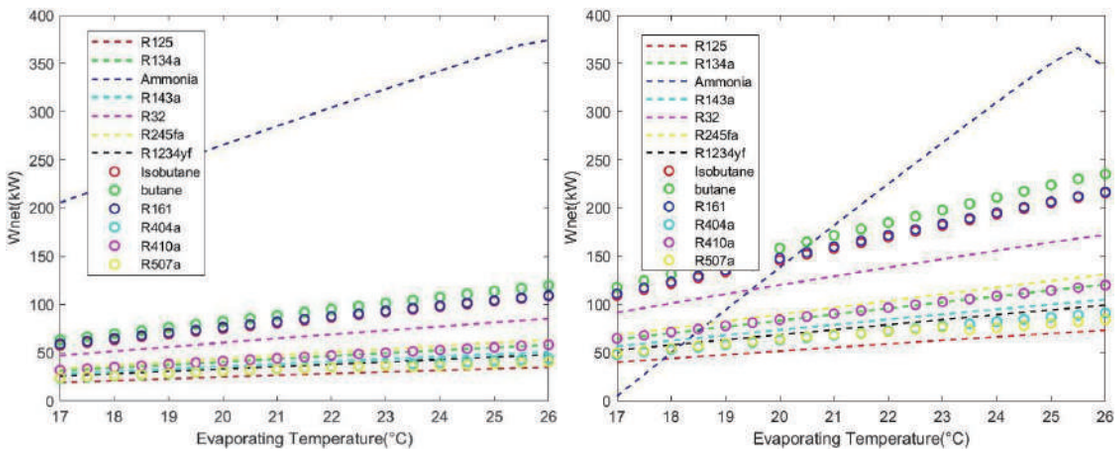

(b) d_w = 2.0 m

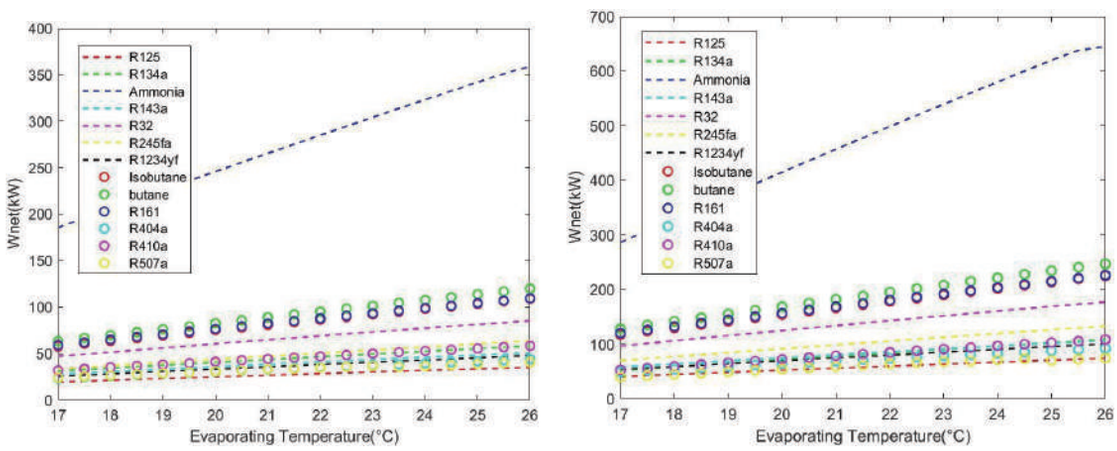

(c) d_w = 2.5 m

Figure 9. Seawater pipe diameter analysis using m_r = 7.117 kg/s (left) and m_r = 15 kg/s (right).

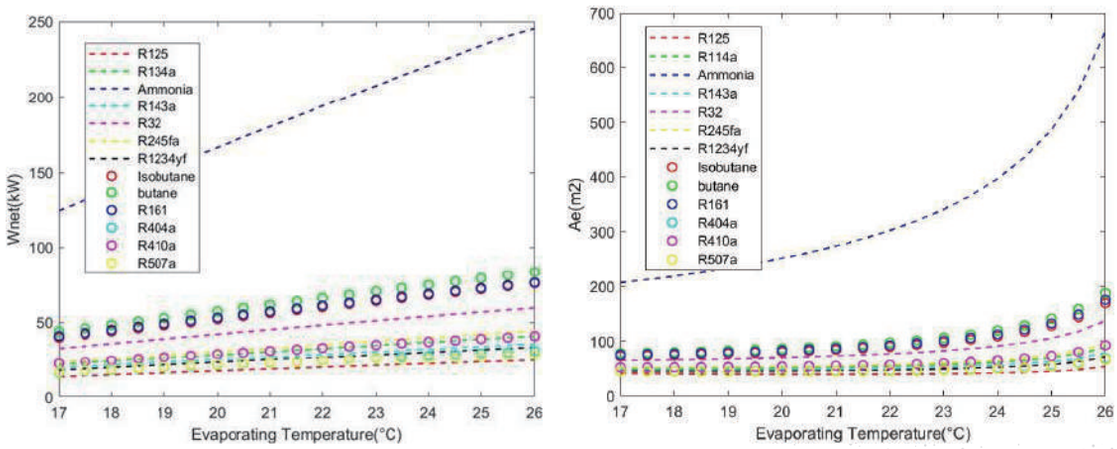

(a) m_r = 5 kg/s

DOI: 10.29677/MR.202412_4(2).0003

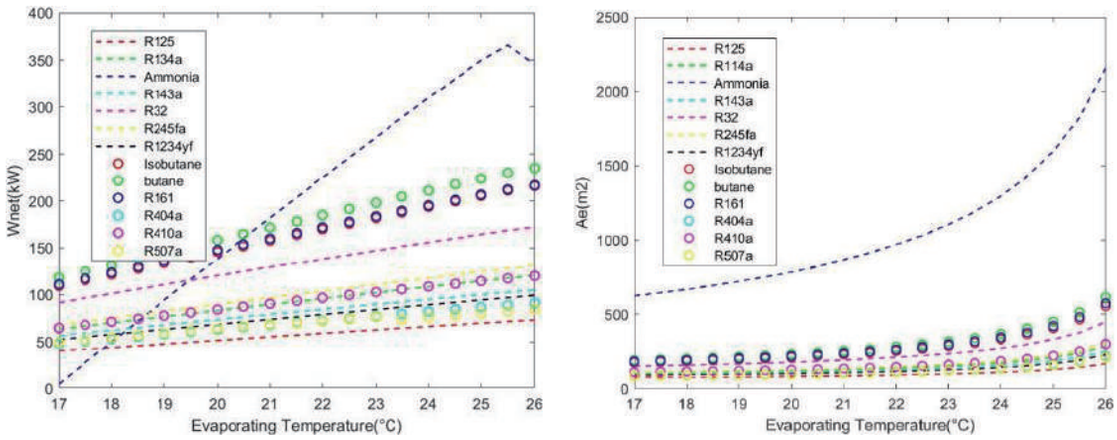

(b) m_r = 15 kg/s

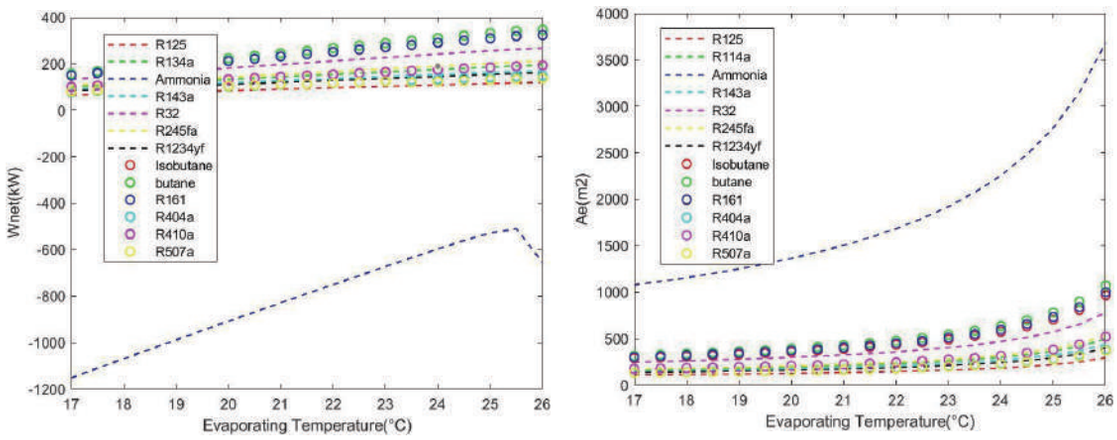

(c) m_r = 25 kg/s

Figure 10. The effect of different mass flow rates on the system's net power (left) and evaporator area (right).

4.3 Performance and Economic Analysis of DORC Working Fluids

Based on the analysis shown in Figures 8 to 10 and Table 2, R134a, R410a, and R507a were selected for their superior net power output and A1 safety classification. Alternatives such as R161, isobutane, and butane were initially considered but excluded due to flammability risks. Although R134a, R410a, and R507a have higher GWPs, their environmental impact can be mitigated through proper maintenance and leak control. The analysis also compares these fluids with ammonia to evaluate their overall suitability.

Marine Research of the National Academy of Marine Research
DOI: 10.29677/MR.202412_4(2).0003

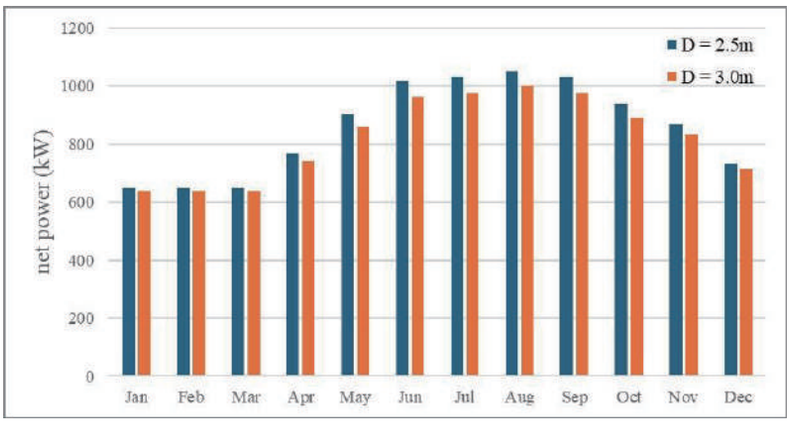

Figure 11. R134a average net monthly power.

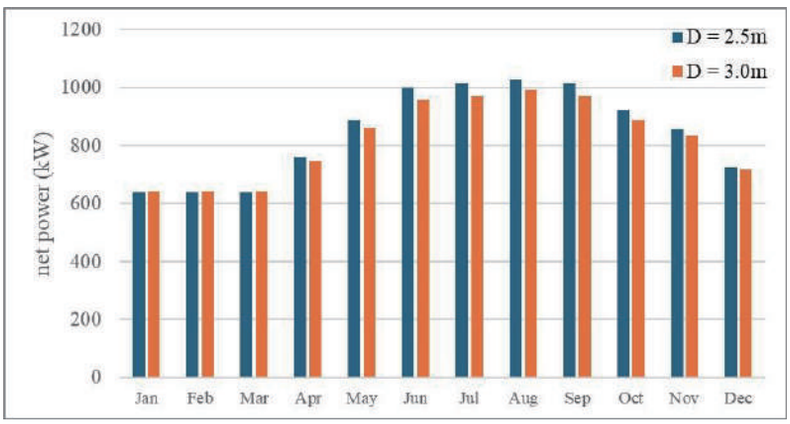

Figure 12. R410a average net monthly power.

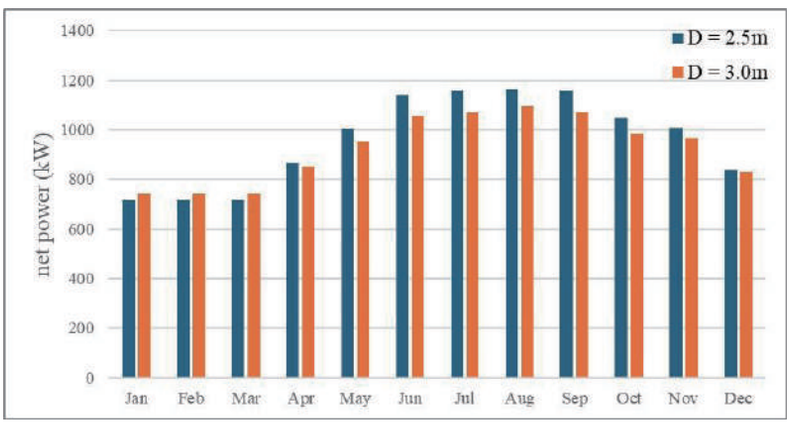

Figure 13. R507a average net monthly power.

Marine Research of the National Academy of Marine Research
DOI: 10.29677/MR.202412_4(2).0003

4.3.1 Net power output for each working fluid

The net power output for the selected working fluids is analyzed under varying monthly operating conditions, providing critical insights into the system's stability and efficiency across different seasonal scenarios. Figures 11 to 13 show the monthly average net power output, highlighting fluctuations throughout the year and underscoring the importance of optimizing the working fluid parameters to enhance performance. A comparative analysis was conducted between pipe diameters of 2.5 m and 3.0 m, as these dimensions demon strated the capacity to achieve a net power output of 1 MW, making them viable design options.

4.3.2 Working fluid performance parameters

This subsection extends the evaluation of performance parameters for various working fluids, building on the previously calculated net power outputs. Table 7 summarizes the OTEC performance parameters for ammonia and the selected working fluids (R134a, R410a, and R507a) at pipe diameters of 2.5 m and 3.0 m.

Both diameters were analyzed for ammonia, but the 2.5 m diameter was chosen for comparison. As shown in Figure 14, ammonia consistently achieved a net power output exceeding 1 MW across a range of evaporating temperatures with a 2.5 m diameter, establishing it as a reliable performance benchmark. While the 3.0 m diameter was also examined, the 2.5 m pipe provided a more optimal balance between performance and design efficiency, particularly in relation to mass flow rate. Therefore, the comparison focuses on ammonia's performance with a pipe diameter of 2.5 m.

In contrast, R134a, R410a, and R507a showed similar net power outputs at 2.5 m and 3.0 m diameters. Figure 14 uses R134a as a representative example to illustrate this consistency. Further analysis is needed to determine the most suitable pipe diameter for each working fluid under the specified operating conditions.

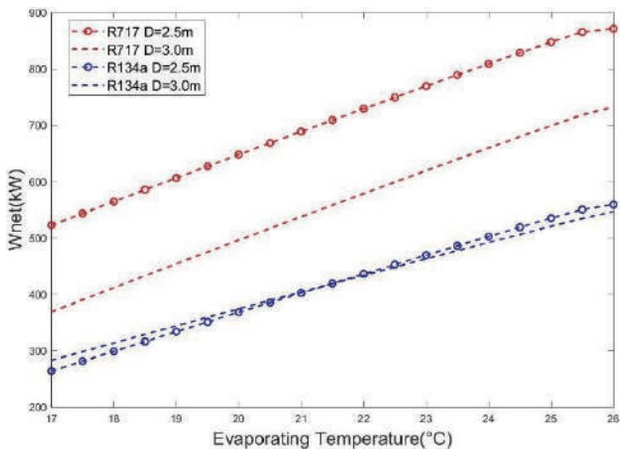

Figure 14. R717 and R134a net power.

Marine Research of the National Academy of Marine Research
DOI: 10.29677/MR.202412_4(2).0003

Table 7. Performance parameters for different working fluids under different pipeline diameters.

Working fluid	γ	η_{ex}	ηOTEC	WPSF	BWR
Ammonia	0.154	0.039	0.029	0.050	0.175
R134a D=2.5m	0.160	0.039	0.030	0.051	0.167
R134a D=3.0m	0.179	0.043	0.033	0.055	0.087
R410a D=2.5m	0.149	0.036	0.028	0.047	0.242
R410a D=3.0m	0.169	0.040	0.032	0.052	0.155
R507a D=2.5m	0.118	0.029	0.024	0.038	0.375
R507a D=3.0m	0.160	0.038	0.031	0.050	0.180

As shown in Table 7, R134a performed optimally at a 3.0 m diameter, achieving higher net power output, superior thermal efficiency, and a lower BWR. These attributes position R134a as the most favorable fluid for larger-diameter systems, delivering significant gains in overall system performance. In contrast, while R410a also improved performance at a 3.0 m diameter, its higher BWR may undermine its economic efficiency despite its strong net power output. Finally, R507a underperformed relative to the other fluids, particularly at smaller diameters, where its net power output and thermal efficiency were markedly lower.

When comparing ammonia to other working fluids such as R134a, the net power output per unit area of ammonia is similar to that of R134a at a diameter of 2.5 m. However, its advantages diminish at larger diameters. Although ammonia achieves comparable thermal efficiency to R134a, its slightly higher BWR may increase operational costs. Overall, R134a holds a slight advantage over ammonia in thermal efficiency and BWR, leading to more favorable economic outcomes for OTEC systems.

4.3.3 Economic analysis of each working fluid

While a 3.0 m diameter system demonstrates superior technical performance, it may also increase construction and operational costs. This subsection presents a comparative economic analysis of the 2.5 m and 3.0 m pipe diameter configurations, considering key cost drivers such as evaporator and condenser areas, as well as pipe length requirements. The design of the DORC system is illustrated in Figures 15 to 17, which serve as the basis for calculating the LCOE for each working fluid. By adjusting system parameters to maximize net power output and minimize operational costs, this analysis facilitates the selection of the most cost-effective fluid for the OTEC system.

DOI: 10.29677/MR.202412_4(2).0003

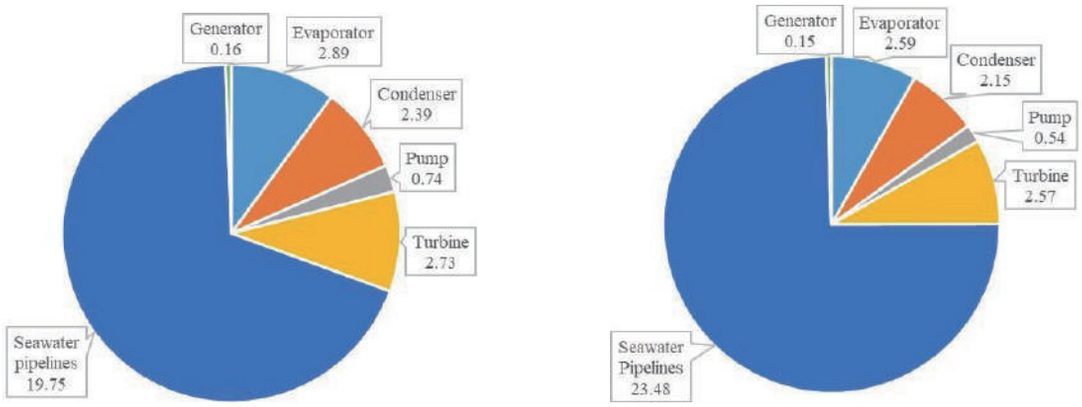

(a) (b)

Figure 15. R134a schematic diagrams of (a) D = 2.5 m and (b) D = 3.0 m.

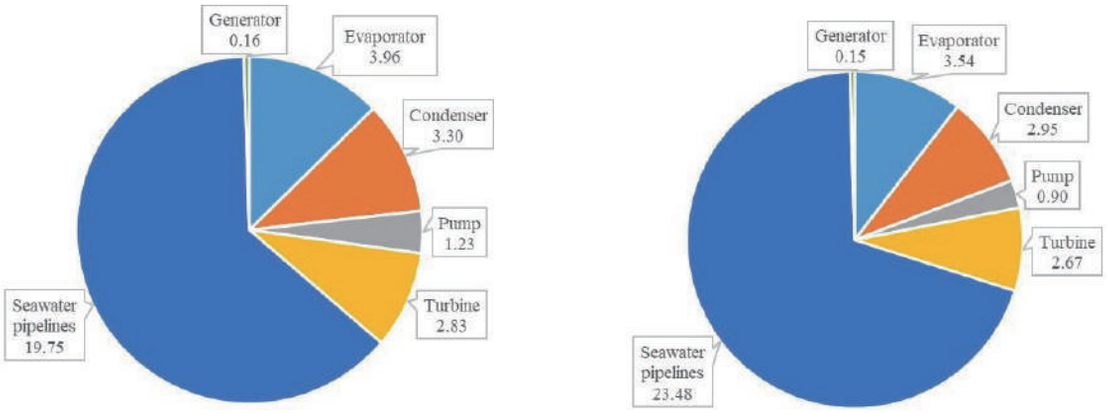

(a) (b)

Figure 16. R410a schematic diagrams of (a) D = 2.5 m and (b) D = 3.0 m.

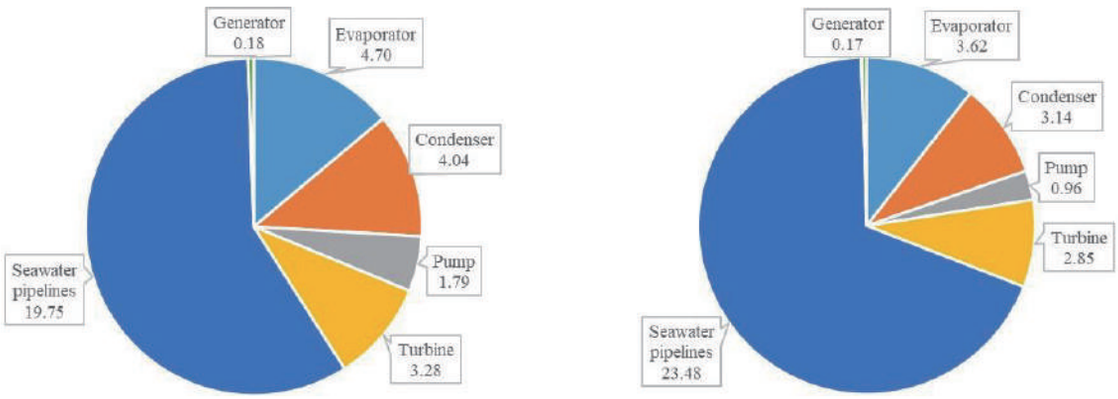

(a) (b)

Figure 17. R507a schematic diagrams of (a) D = 2.5 m and (b) D = 3.0 m.

DOI: 10.29677/MR.202412_4(2).0003

4.4 Comprehensive Assessment

The LCOE was calculated using Eq. 17 based on the cost data presented in Figures 15–17, with the outcomes listed in Table 8. These results are integrated with the performance parameters to comprehensively analyze the technical and economic performance of various pipe diameter configurations and working fluids. This systematic comparison facilitates a robust assessment of the feasibility of the OTEC system under different operational conditions.

Table 8. Performance parameters and LCOE.

Working fluid	γ	η_{ex}	η_{OTEC}	WPSF	BWR	LCOE (USD/kW)
Ammonia	0.154	0.039	0.029	0.050	0.175	0.371
R134a D = 2.5 m	0.160	0.039	0.030	0.051	0.167	0.405
R134a D = 3.0 m	0.179	0.043	0.033	0.055	0.087	0.464
R410a D = 2.5 m	0.149	0.036	0.028	0.047	0.242	0.448
R410a D = 3.0 m	0.169	0.040	0.032	0.052	0.155	0.496
R507a D = 2.5 m	0.118	0.029	0.024	0.038	0.375	0.426
R507a D = 3.0 m	0.160	0.038	0.031	0.050	0.180	0.449

Table 8 indicates that the LCOE is higher for an OTEC system with a 3.0 m pipe diameter compared to one with a pipe diameter of 2.5 m, primarily due to increased pipeline costs. Although reductions in evaporator and condenser surface area costs are observed, they do not sufficiently offset the rise in pipeline expenses. Consequently, the analysis focuses on the LCOE for an OTEC system with a 2.5 m pipe diameter. At a net power output of 1 MW, the LCOE is approximately 0.45 USD/kW (Christodoulides et al., 2023), which is considered acceptable for a 2.5 m diameter system. R134a emerges as the most favorable alternative to ammonia, demonstrating strong efficiency, economic viability, and enhanced environmental sustainability due to its lower global warming potential. Therefore, it is recommended as the preferred working fluid for this study.

5 CONCLUSIONS

This study comprehensively analyzed the selection of working fluids and system performance for OTEC technology. By modeling a DORC and using seawater temperature data from the Heping area in Hualien, Taiwan, the performance of the OTEC system with 13 working fluids was simulated and systematically compared. The findings reveal that R134a surpasses ammonia in terms of thermal efficiency and economic viability, particularly demonstrating notable advantages in BWR and net power output. Despite these benefits, the overall cost of systems utilizing R134a remains higher than those using ammonia. Nevertheless, this research underscores the importance of optimizing both the selection of working fluids and design parameters, such as seawater pipe diameter and pinch point temperature, to significantly enhance the power generation efficiency of OTEC systems while concurrently reducing construction costs. Future research should concentrate on further improving thermal efficiency, enhancing safety measures, and minimizing operational costs to facilitate the development of OTEC technology as a sustainable renewable energy solution.

DOI: 10.29677/MR.202412_4(2).0003

REFERENCES

Alkhalidi, A., Qandil, M., & Qandil, H. (2014). Analysis of OTEC power plant using isobutane as the working fluid. *International Journal of Thermal and Environmental Engineering, 7*(1), 25-32. https://doi.org/10.5383/ijtee.07.01.004

Aresti, L., Christodoulides, P., Michailides, C., & Onoufriou, T. (2023). Reviewing the energy, environment, and econ- omy prospects of ocean thermal energy conversion (OTEC) systems. *Sustainable Energy Technologies and Assessments, 60,* 103459. https://doi.org/10.1016/j.seta.2023.103459

Central Weather Administration. (2024, August 14). *Sea Surface Temperature Statistics.* Climate - Central Meteorological Administration Global Information Network. Retrieved September 30, 2024, from https://www.cwa.gov.tw/V8/C/C/MMC_STAT/sta_sea.html

Chen, W., & Huo, E. (2023). Opportunities and challenges of ocean thermal energy conversion technology. *Frontiers in Energy Research, 11.* https://doi.org/10.3389/fenrg.2023.1207062

Dijoux, A., Sinama, F., Marc, O. M., Clauzade, B., & Castaing-Lasvignottes, J. (2017). Working fluid selection general method and sensitivity analysis of an organic Rankine cycle (ORC): Application to ocean thermal energy conversion (OTEC). *HAL Open Science,* hal-01653074. https://hal.science/hal- 01653074

Gu, Y. (2023). A key parameter in design and operation of ocean thermal energy conversion plants. *Proceedings of the 8th Thermal and Fluids Engineering Conference (TFEC),* USA, 693-702. https://doi.org/10.1615/TFEC2023.eet.045114

Halimi, B., & Atolah, R. Y. (2019). Analysis of 100 kW ocean thermal power plant with butene as working fluid. *IOP Conference Series: Earth and Environmental Science, 339,* 012039. https://doi.org/10.1088/1755-1315/339/1/012039

Halimi, B., Atolah, R. Y., Julianti, E., & Kastawan, I. M. W. (2020). Working fluid candidates selection for 100kw ocean thermal power generation based on environmental, safety, and thermodynamic constrains. *TELKA - Telekomunikasi Elektronika Komputasi dan Kontrol, 6*(1), 20–28. https://doi.org/10.15575/telka.v6n1.20-28

Ikegami, Y., Yasunaga, T., & Morisaki, T. (2018). Ocean thermal energy conversion using double-stage Rankine cycle. *Journal of Marine Science and Engineering, 6*(1). https://www.mdpi.com/2077-1312/6/1/21

Kempener, R., & Neumann, F. (2014). *Ocean thermal energy conversion: Technology brief.* International Renewable Energy Agency. https://www.irena.org/Publications/2014/Jun/Ocean-Thermal-Energy-Conversion

Kim, N. J., Ng, K. C., & Chun, W. (2009). Using the condenser effluent from a nuclear power plant for ocean thermal energy conversion (OTEC). *International Communications in Heat and Mass Transfer, 36*(10), 1008–1013. https://doi.org/10.1016/j.icheatmasstransfer.2009.08.001

Kusuda, E., Morisaki, T., & Ikegami, Y. (2015). Performance test of double-stage Rankine cycle experimental plant for OTEC. *Procedia Engineering, 105,* 713–718. https://doi.org/10.1016/j.proeng.2015. 05.061

DOI: 10.29677/MR.202412_4(2).0003

Langer, J., Infante Ferreira, C., & Quist, J. (2022). Is bigger always better? designing economically feasible OTEC systems using spatiotemporal resource data. *Applied Energy, 309,* 118414. https://doi.org/10.1016/j.apenergy.2021.118414

Lemmon, E. W., Huber, M. L., & McLinden, M. O. (2013). *NIST reference fluid thermodynamic and transport properties – REFPROP (Version 9.1 User's Guide).* National Institute of Standards and Technology. https://www.nist.gov/system/files/documents/srd/REFPROP9.PDF

Liponi, A., Baccioli, A., Vera, D., & Ferrari, L. (2022). Seawater desalination through reverse osmosis driven by ocean thermal energy conversion plant: Thermodynamic and economic feasibility. *Applied Thermal Engineering, 213*, 118694. https://doi.org/10.1016/j.applthermaleng.2022.118694

Makai Ocean Engineering. (n.d.). *Ocean thermal energy conversion (OTEC)*. Makai's OTEC projects. Retrieved September 30, 2024, from https://www.makai.com/renewable-energy/otec/

OTEC Okinawa. (n.d.). *Okinawa ocean thermal energy conversion demonstration test facility.* Retrieved September 26, 2024, from http://otecokinawa.com/en/

Renewable Energy Sources. (2009, October 27). *Open cycle ocean thermal energy conversion (OTEC).* https://newenergyportal.wordpress.com/2009/10/27/open-cycle-ocean-thermal-energy-conversion-otec/

Saleh, B., Koglbauer, G., Wendland, M., & Fischer, J. (2007). Working fluids for low-temperature organic Rankine cycles. *Energy, 32*(7), 1210–1221. https://doi.org/10.1016/j.energy.2006.07.001

Taiwan Power Company. (n.d.). *Proportion of electricity generation and purchase over the years.* Taiwan Power Company. Retrieved November 10, 2017, from https://www.taipower.com.tw/2289/2363/2367/2372/10312/

Toffolo, A., Lazzaretto, A., Manente, G., & Paci, M. (2014). A multi-criteria approach for the optimal selection of working fluid and design parameters in organic Rankine cycle systems. *Applied Energy, 121,* 219–232. https://doi.org/10.1016/j.apenergy.2014.01.089

Turton, R., Bailie, R. C., Whiting, W. B., & Shaeiwitz, J. A. (Eds.). (2009). *Analysis, synthesis, and design of chemical processes* (3rd ed.). Prentice Hall.

Wei, J. G. (2023, April 21). *Opportunities and challenges for the development of thermoelectric energy industry* [Panel Discussion]. 2023 The First Ocean Energy Industry Development Forum, Taiwan.

Yang, M. H., & Yeh, R. H. (2014). Analysis of optimization in an OTEC plant using organic Rankine cycle. *Renewable Energy, 68*, 25–34. https://doi.org/10.1016/j.renene.2014.01.029

Yang, M. H., & Yeh, R. H. (2022). Investigation of the potential of R717 blends as working fluids in the organic Rankine cycle (ORC) for ocean thermal energy conversion (OTEC). *Energy, 245.* https://doi.org/10.1016/j.energy.2022.123317

Yang, X., Liu, Y., Chen, Y., & Zhang, L. (2022). Optimization design of the organic Rankine cycle for an ocean thermal energy conversion system. *Energies, 15*(18). https://doi.org/10.3390/en15186683

Yoon, J. I., Son, C. H., Baek, S. M., Kim, H. J., & Lee, H. S. (2014). Efficiency comparison of subcritical OTEC power cycle using various working fluids. *Heat and Mass Transfer, 50*(7), 985–996. https://doi.org/10.1007/s00231-014-1310-8